

# Overcoming Interfacial Affinity Issues in Natural Fiber Reinforced Polylactide Biocomposites by Surface Adsorption of Amphiphilic Block Copolymers

Kevin Magniez,<sup>†,\*</sup> Andreea S. Voda,<sup>†</sup> Abdullah A. Kafi,<sup>†</sup> Audrey Fichini,<sup>†,‡</sup> Qipeng Guo,<sup>†</sup> and Bronwyn L. Fox<sup>†</sup>

<sup>†</sup>Institute for Frontier Materials, Deakin University, Victoria, Waurn Ponds, 3217, Australia

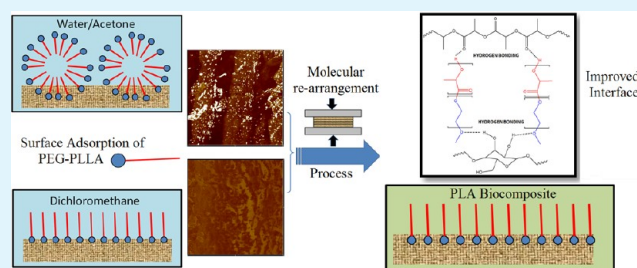
<sup>‡</sup>École nationale supérieure des arts et industries textiles (ENSAIT), Roubaix, 59056, France

## Supporting Information

**ABSTRACT:** This work demonstrates that the interfacial properties in a natural fiber reinforced polylactide biocomposite can be tailored through surface adsorption of amphiphilic and biodegradable poly (ethylene glycol)-*b*-poly (L-lactide) (PEG-PLLA) block copolymers. The deposition from solvent solution of PEG-PLLA copolymers onto the fibrous substrate induced distinct mechanisms of molecular organization at the cellulosic interface, which are correlated to the hydrophobic/hydrophilic ratios and the type of solvent used. The findings of the study evidenced that the performance

of the corresponding biocomposites with polylactide were effectively enhanced by using these copolymers as interfacial coupling agents. During the fabrication stage, diffusion of the polylactide in the melt induced a change in the environment surrounding block copolymers which became hydrophobic. It is proposed that molecular reorganization of the block copolymers at the interface occurred, which favored the interactions with both the hydrophilic fibers and hydrophobic polylactide matrix. The strong interactions such as intra- and intermolecular hydrogen bonds formed across the fiber–matrix interface can be accounted for the enhancement in properties displayed by the biocomposites. Although the results reported here are confined, this concept is unique as it shows that by tuning the amphiphilicity and the type of building blocks, it is possible to control the surface properties of the substrate by self-assembly and disassembly of the amphiphiles for functional materials.

**KEYWORDS:** interfacial interaction, surface adsorption, amphiphile, biocomposites, polylactide, natural fibers



## INTRODUCTION

Government regulations and growing environmental awareness throughout the world are driving the move towards the design of composite materials manufactured from eco-friendly and renewable materials. With this mind set, the use of natural fibers as a potential alternative reinforcement to synthetic fibers is particularly desirable for the development of environmentally sustainable materials. The advantageous balance of properties displayed by ligno-cellulosic fibers (such as kenaf, hemp, jute, and flax) in terms of density, modulus and light weight has earned them a predominant role in some nonstructural interior automotive components.<sup>1,2</sup> However, these materials were traditionally designed using petroleum-derived resins (such as polyolefin), which seriously jeopardize their sustainability.

Over the past few years, the combination of natural fibers and renewable polymers to produce bio-composite materials has generated some considerable momentum as a result of recent advances of the mass synthesis of biopolymers. Amongst them is polylactic acid (PLA), an aliphatic polyester thermoplastic derived from corn starch or sugarcane. Because of its appealing biodegradability, materials based on PLA in combination with natural fibers have since been developed

and commercialized.<sup>3,4</sup> However, the poor quality of the interface between the hydrophilic reinforcing fibers and the hydrophobic PLA matrix underpins the poor performance displayed by these materials.<sup>5</sup>

To date, the research in this field is still strongly focused on improving their interfacial properties, which are inevitably related to their general and long-term performances.<sup>6</sup> Interfacial compatibility issues have been gradually overcome through chemical surface modification of the fibers using alkali, silane or acetylation treatment<sup>7</sup> and physical surface treatment such as plasma.<sup>8</sup> Scientifically, a number of publications by Graupner,<sup>9–12</sup> Plackett,<sup>13</sup> Huda,<sup>14</sup> and Hu<sup>15,16</sup> have addressed some of these issues. Of particular relevance here is the work reported by Graupner. The author found that the interfacial properties in cellulosic cotton fiber reinforced PLA biocomposites were weaker compared to their counterpart materials made using ligno-cellulosic hemp and kenaf fibers.<sup>10</sup> In a subsequent publication, Graupner improved the interfacial and

Received: September 16, 2012

Accepted: December 20, 2012

Published: December 20, 2012

mechanical properties of cotton fiber reinforced PLA by purposely adding a small amount of lignin, thus proving that the lignin present on the outer surface of ligno-cellulosic fibers, is acting as a coupling agent thus improving the interfacial adhesion.<sup>9</sup> In more recent times, John et al. presented a study on the use of zein-protein from corn as an amphiphilic coupling agent in Kenaf–polypropylene composites, showing some modest improvements in tensile and flexural modulus after treatment.<sup>17</sup>

The work presented herein draws on this concept by investigating the possibility of overcoming interfacial affinity issues in a jute and polylactide biocomposite by using amphiphilic block copolymers which can be designed to compatibilize both interfaces. Because poly(ethylene glycol) (PEG) has previously demonstrated strong hydrogen bonding interaction with cellulose<sup>18</sup> and poly(L-lactide) (PLLA) is for obvious reasons compatible with polylactide, we proposed the use of poly(ethylene glycol)-b-poly(L-lactide) (PEG-PLLA) block copolymers for this purpose. This research paper will investigate the deposition from solvent solution and surface adsorption onto the jute substrate of PEG-PLLA copolymers of various hydrophobic/hydrophilic ratios. The molecular organization of the copolymers at the cellulosic interface will be discussed in detail. The effect of surface adsorption of the block copolymers on the properties of the corresponding biocomposites with PLA is reported in terms of flexural, thermo-mechanical and impact performance. We focussed on understanding and interpreting the nature of the interactions at the fiber–matrix interface in order to fully understand the mechanism responsible for the changes in properties.

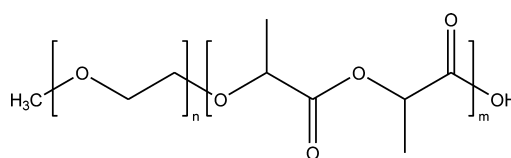
## EXPERIMENTAL SECTION

**Materials.** A plain weave of raw and unbleached jute (*Corchorus* genus) of approximately 350 gram per square meter was obtained from Bangladesh Jute Mills Corporation, Dhaka. Polylactic acid films (300 micrometers thickness) were purchased from Bi-Ax international (Canada). L-Lactide, poly(ethylene glycol) methyl ether (MPEG) ( $M_n \approx 5000$ ), and stannous octoate  $\text{Sn}(\text{Oct})_2$  were purchased from Sigma-Aldrich. Analytical grades diethyl ether, dichloromethane, and toluene were purchased from Chem-Supply and Ajax Finechem.

**Synthesis of the PEG-PLLA Block Copolymers.** L-Lactide was first recrystallised from acetone, then dried in vacuo at 60 °C for 12 h along with MPEG. The MPEG polymer and L-lactide monomer were then added to a dried Schlenk tube, blanketed with argon and heated to 130 °C. The  $\text{Sn}(\text{Oct})_2$  catalyst (0.15 w/v in freshly distilled toluene) was added and the reaction was allowed to occur at 130 °C, under argon, over a period of 12 h. The reaction product was then dissolved in DCM and twice recrystallised from ice cooled diethyl ether. The isolated product was dried in vacuo prior to analysis. A molar ratio of 1:1000 of  $\text{Sn}(\text{Oct})_2$  to L-lactide monomer was used and the molecular weight of the PLLA blocks was varied by changing the feed of L-lactide monomer (whilst maintaining a fixed PEG molecular weight of 5000 g/mol). Three types of block copolymers (BCP) were produced with PEG to PLLA ratios of 2:1, 1:1 and 1:2 (see Table 1). The molecular weights were estimated using <sup>1</sup>H Nuclear Magnetic Resonance Spectroscopy (NMR) (see the Supporting Information, SI1) through integration of the methylene peak ( $-\text{O}-\text{CH}_2-\text{CH}_2-$ ) of the PEG block observed at  $\delta \approx 3.64$  ppm to the proton at  $\delta \approx 5.17$  ppm ( $\text{CH}_3-\text{CH}^* <$ ) of the PLLA block. The polydispersity indices measured by gel permeation chromatography were between 1.02 and 1.49.

**Surface Treatment of the Jute Substrate.** To remove the waxy substances and other contaminants from the surface of the jute, the woven fabrics were cleaned in a bath of sodium hydroxide (2 g/L), Clariant Imerol XNA (1 g/L) and de-ionized water at 80 °C during 30 min under stirring (1/20 liquor ratio). The samples were then washed

**Table 1. Types of Synthesized (PEG-PLLA) Block Copolymers (BCP)**



type	2:1 PEG/ PLLA ratio ( $m = 2n$ )	1:1 PEG/ PLLA ratio ( $m = n$ )	1:2 PEG/ PLLA ratio ( $2m = n$ )
terminology	BCP1	BCP2	BCP3
estimated $M_w$ (g/mol)	7500	9300	16 100

in hot water (50 °C), neutralized in weak acetic acid solution (0.2 g/L) and washed again twice in hot water (50 °C).

The alkali-treated fabrics were surface coated with 3 and 5 wt % of each copolymer. The first step involved looking at the solubility of each copolymer using a variety of solvents; water, acetone, and dichloromethane were chosen (Table 2). Fabrics absorbed individual solvent mixtures differently and therefore solvent uptake was calculated for each mixture by taking the average weight absorbed by the dry alkali treated jute fabric after dipping the fabric into a glass beaker filled with a large quantity of the solvent. Surface treatment was carried out by dipping square samples of dry alkali treated fabrics of known dimensions and mass (~11 g, 120 mm in length) into the solvent solution containing various concentrations of copolymer.

**Characterization of the Physicochemical Properties of the Jute.** The cohesive tensile properties of jute yarns extracted by hand from the woven fabric (minimum of 10, in both weft and warp direction) were tested using a Lloyd LR30 K using an extension of 2 mm/min over an effective gauge length of 80 mm with a pretension of 0.5cN/tex. The yarn linear density (tex) was used to normalize the force values resulting from each test and specific stress (cN/tex) versus extension (mm) curves were determined.

The microstructural and chemical changes of the jute fibers were measured before and after surface treatment using a Vertex Infrared Spectrometer (Bruker Optics Inc., Germany) in the attenuated total reflectance (ATR) mode equipped with a germanium crystal (Pike Technologies, USA). A total of 64 measurements were obtained directly onto the fibers at a scan resolution of 4  $\text{cm}^{-1}$  between 4000 and 600  $\text{cm}^{-1}$ . The spectrum was normalized at 895  $\text{cm}^{-1}$  ( $\text{C}_1$  group frequency of the  $\beta$ -glucosidic linkage).

**Self-Assembly in Solution.** Dynamic light scattering (DLS) measurements were performed with a Malvern Zetasizer Nano ZS spectrometer equipped with 4mW He–Ne laser (emission 633 nm). All measurements were carried out at 25 °C using noninvasive backscatter (NIBS) optics with a detection angle of 173°. Analysis was performed using solution  $S_1$  prepared using Mili-Q water and acetone at the same concentrations as those described in Table 2. Each sample was filtered through a syringe filter (0.45  $\mu\text{m}$  pore size) prior to measurement. The size distribution histogram reported in this paper are the z-average diameters measured by the instrument using cumulative analysis.

**Atomic Force Microscopy (AFM).** Atomic force microscopy was used to investigate the micro and nano-structural organization of the block copolymers on the surface of the alkali treated jute fibers after deposition and surface adsorption from solvent solution. The fibers were extracted delicately by hand from the treated fabric. The fibers were then dried overnight at 65 °C in vacuo prior to analysis. A minimum of 3 fiber samples (approximately 20 mm in length) were placed flat and straight on thin microscope coverslips (22 × 22 mm) on which double side tape has been fixed. The coverslip was then analyzed using a tapping mode Digital Instruments Dimension 3000 SPM in air under ambient conditions using a Bruker TESPW AFM probe with a spring constant of 42 N/m. Tapping mode amplitude and phase images were captured with a scan rate of 1 Hz from 4 spots over 2 separate single fiber. The amplitude image records the topography of the surface whilst the phase image depicts shifts in the phase angle of

Table 2. Solvent Mixtures (with ratios) Used to Prepare Copolymer Solution

copolymer	solvent	wt % of solvent absorbed by the fabric	copolymer concentration (mg/mL)	terminology of the solution
BCP1	1:1 water/acetone	69	11.5	S <sub>1</sub>
BCP1	1:1 water/acetone	69	20	S <sub>1</sub> '
BCP2	dichloromethane	48	17	S <sub>2</sub>
BCP2	dichloromethane	48	28.4	S <sub>2</sub> '
BCP3	1:2 water/acetone	66	11	S <sub>3</sub>
BCP3	1:2 water/acetone	66	18.4	S <sub>3</sub> '

the probe oscillation as a consequence of tip/surface interactions. Under the right conditions, phase imaging can be used to highlight the presence of multiple phases.<sup>19</sup>

**Fabrication of the Biocomposite.** The jute fabrics previously prepared were then used to produce a number of composite samples in combination with polylactide (PLA). In order to minimize hydrolysis of the polymer chains caused by a combination of moisture and heat, both the PLA films and fabrics samples were dried overnight in vacuo at 70 °C prior to processing. The composites were produced by compression molding via a stacking procedure using square samples of fabrics (120 mm in length). The stacking sequence was achieved by alternating four layers of fabrics (placed with a [0/90] orientation in both warp and weft directions) with five layers of PLA films. Two thermocouples were inserted one on each side of the laminate before vacuum bagging to record temperature. The stack was carefully placed into a stainless steel coated mold with a release agent. The assembly was vacuum bagged at 85 kPa and placed in a hot press at 175 °C for 20 min. Pressures of 1, 1.5, and 2.5 MPa were applied for 10, 5, and 2 min, respectively. Polylactide can undergo hydrolysis as a result of residual moisture combined with high processing temperatures. The changes in the molecular weight of the polylactide matrix before and after thermal processing was characterised by gas phase chromatography. No significant change in the molecular weight of the polylactide was measured using these processing conditions (see the Supporting Information, SI2). The composites were removed from the press, debagged, and immediately annealed in a conventional oven at 110 °C for 30 min.

**Mechanical Characterization of the Biocomposites.** Dynamic mechanical analyses (DMA) were performed using a Q800 instrument equipped with a dual-cantilever bending flexural loading mode at a frequency of 1 Hz with a constant strain of 0.05% and a heating rate of 2 °C/min between 0 and 125 °C. Specimens of approximate dimensions of 55 mm × 12 mm × 2 mm were used. Flexural strength and flexural modulus were determined using the 3 point bending method as per ASTM D790-84a with a span length of 16 times the thickness and a crosshead speed of 2 mm/min using a Lloyd LR30 K universal tensile tester. All tests were conducted at 20 ± 2 °C and 65 ± 2% relative humidity allowing sample conditioning for 48 h prior to the tests. Testing based on the ASTM D256 using type 3 specimens of approximate dimensions of 32 mm × 10 mm × 2 mm was carried out. The impact energy was measured with a pendulum length of 200 mm and with an energy of 10 Joules on un-notched specimens in the edgewise direction.

## RESULTS AND DISCUSSION

### Microstructural and Physical Properties of the Fibers.

Following the mild alkaline treatment, scanning electron microscopy images revealed a smooth surface free from contaminants such as wax and pectin (see the Supporting Information, SI3). The microstructural and chemical changes in jute after alkali treatment were detectable from their infrared spectra (Figure 1). Before and after alkaline treatment, the jute fibers exhibited various distinct stretching absorption peaks corresponding to the  $\alpha$ -cellulose, hemicellulose, and lignin major constituents. The relatively unchanged peaks at 1650 cm<sup>-1</sup> ( $\nu_s$  para-substituted C=O) and between 1440 and 1530 cm<sup>-1</sup> showed that the lignin components were not removed

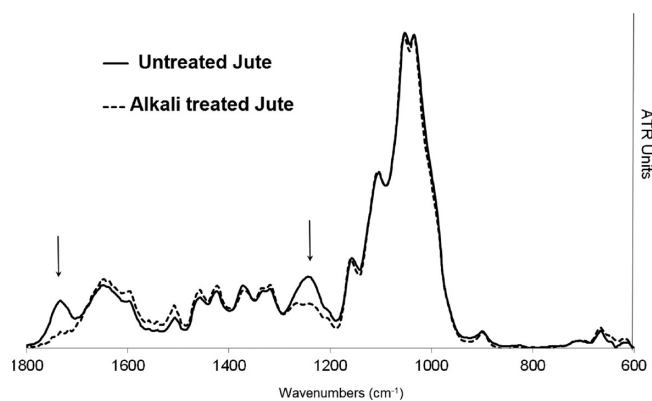


Figure 1. ATR-FTIR spectra of untreated and alkali-treated jute fibers.

during treatment. This is not surprising, as cold alkali treatment using between 0.25 and 20 wt % sodium hydroxide has previously been shown not to dissolve the lignin in jute fibers<sup>20</sup>

On the other hand, the sharp decrease in the intensity of the absorbance peak at 1750 cm<sup>-1</sup> ( $\nu_s$  C=O linkage in acetyl ester group) and at 1250 cm<sup>-1</sup> ( $\delta_s$  CH bending), highlighted by the arrows in Figure 1, suggested that hemicellulose was removed.<sup>21</sup>

The alkaline treatment had a positive effect on the tensile properties of the yarn. Whilst the tenacity and modulus (Figure 2) were not affected (which is consistent with refs 22 and 23), the values of elongation at break were found to increase by up

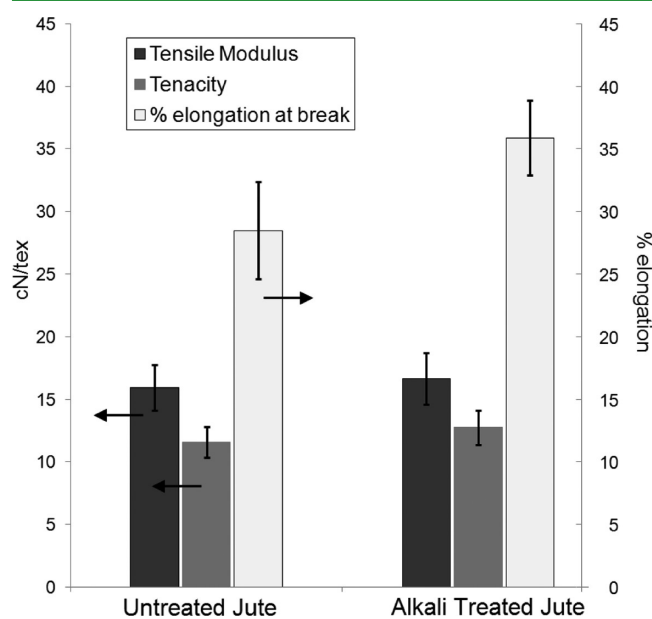


Figure 2. Tensile properties of the untreated jute fibers and alkali-treated jute fibers.

to 50%. This trend can be explained from the removal of hemicelluloses contained within the interfibrillar regions of the fibers as reported elsewhere.<sup>24</sup> Morphologically, jute fiber contains a number of primary cells which are laterally interconnected by a layer called the middle lamella (primarily composed of pectin and lignin). Each primary cell wall contains a network of long cellulosic fibrils embedded in hemicelluloses and lignin. It has been reported that as the hemicellulose is dissolved, swelling and shrinkage of the ultimate cells occur, resulting in the loosening of the interfibrillar region.<sup>24</sup> This mechanism is likely to improve the extension at break due to the ability of the microfibrils to rearrange during tensile loading and increase stress transfer between the fibrils.

**Interfacial Analysis.** We investigated the changes in the surface properties of the fibers after adsorption of the amphiphilic block copolymers. This will help us understand and interpret the nature of the interactions at the fiber-matrix interface which will be useful in intercorrelating the mechanism responsible for the changes in physical properties reported later in this paper.

The surface adsorption of the block copolymers mechanism from water/acetone mixtures ( $S_1$ ,  $S_1'$ ,  $S_3$ , and  $S_3'$ ) was expected to be different from that of dichloromethane mixtures ( $S_2$  and  $S_2'$ ). In the particular case of water/acetone as a solvent, concentrations of several grams per liter were used to dissolve BCP1 and BCP3 block copolymers, which exceeds the critical micelle concentration.<sup>25</sup> Above this concentration and in aqueous milieu, the formation of spherical micelles with an hydrophilic PEG shell with an inner PLLA core is expected.<sup>26</sup> On the other hand, micelle formation was not expected in solutions  $S_2$  and  $S_2'$  simply because dichloromethane is a particularly good cosolvent for both PLLA and PEG blocks.<sup>27</sup> Dichloromethane was selected as a solvent in the early stage of the work to solubilize BCP2 copolymer which was found to be only partially miscible in water/acetone possibly because of strong inter-molecular competitive interactions (as the PEG and PLLA blocks are present in equal ratio).

Dynamic light scattering (DLS) analysis was performed on a selected sample (solution  $S_1$  consisting of BCP1 in water/acetone). The  $z$ -average diameter recorded for the particles was 153.1 nm with a PDI of 0.237. Although the particles measured gave rise to a unimodal distribution centered at 37.7 nm (Figure 3), the histogram was skewed to the right indicating the

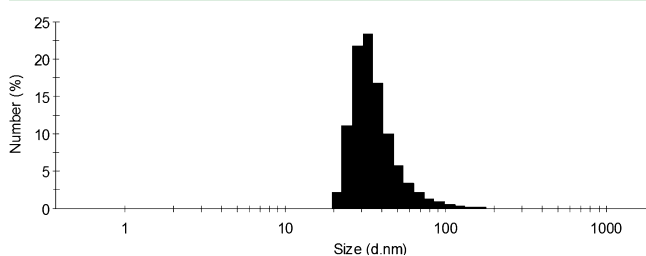


**Figure 3.** Size distribution by number results on  $S_1$  solution containing the block copolymer 1 dissolved in a mixture of water and acetone.

presence of larger aggregates. The large  $z$ -average and PDI values were therefore attributed to the presence in solution of larger self-aggregating particles. Despite self-assembly not being expected to occur in dichloromethane, DLS analysis was also performed on the BCP2 sample as a control. As expected, the sample was polydisperse and presented with large aggregating particles. The formation of polymer clusters occurring from first

association and entanglements of the copolymers is believed to be the cause for these observations<sup>28</sup>

Atomic force microscopy (AFM) was very useful in disclosing the changes in surface topography of the fibers after surface adsorption of the copolymers in solution. We found that the surface of the alkali treated jute fibers (shown in the amplitude image, Figure 4) was relatively smooth and the phase image did not reveal any features of interest here. Upon surface adsorption of the PEG-PLLA BCP1 from acetone/solvent solution  $S_1$  (only shown here as a representative example), the amplitude images revealed the spherical nano-sized features distributed on the surface of the fiber. The phase image confirmed the presence of a separate phase, with discrete micelles (30–50 nm) and self-agglomerated micelles (>100 nm) visible, which correlated with the DLS data.

The surface topography of the jute after surface adsorption with  $S_2$  did not seem to change, but the phase images revealed that the block copolymer was scarcely coated on the surface of the fibers. This is logical since the copolymer was fully solubilized in dichloromethane and therefore one would expect to obtain a monolayer deposition.

**Physical Properties of the Composites.** Biocomposite samples with a polylactide (PLA) matrix were produced using a jute woven substrate which was untreated, alkali-treated, and alkali-treated followed by surface adsorption with the various block copolymer (BCP) solutions listed in Table 2. The flexural properties of the samples are presented in Figure 5, showing an obvious dependence of the surface treatment of jute. The values are within the range reported for natural fibers reinforced composites (typically 3–6 GPa in flexural modulus and 60 to 120 MPa in flexural strength).<sup>14,15,29,30</sup> After surface treatment with the block copolymers, a notable increase in modulus of up to 35% was observed. This result can be correlated to the improvement in interfacial properties of the composites as published elsewhere.<sup>31,32</sup> A more moderate effect on the flexural strength with a maximum increase of 20% was measured after surface adsorption of the copolymers (all within the range of statistical deviation).

Figure 6 shows the effect of the surface treatment of jute on the thermo-mechanical response of the bio-composites. The datum presented supports very well the assumptions of an improvement in interfacial property when the block copolymers are adsorbed on the surface of the jute fibers. The dynamic response ( $E'$ ) of the bio-composites was ameliorated, reflecting on the improved fiber–matrix adhesion as reported elsewhere.<sup>33</sup> Between 0 and 60 °C, the storage modulus was approximately 40% higher using the  $S_3'$  formulation. The storage modulus for the samples treated with the block copolymers consistently followed the same trend, and thus it is reasonable to say that the nature of the interface is preserved over the range of temperature tested.

The height of the tan delta ( $\delta$ ) peak decreased after both the alkali and block copolymers treatments (Figure 6). This result stems from the ability of the material to bear a greater stress through better fiber–matrix adhesion inducing a reduction in molecular mobility at this interface. Very importantly, it can be highlighted that concentration had an overpowering effect over the hydrophobic/hydrophilic ratios of the block copolymers. It can be seen that the increase in storage modulus and the decrease in the height of the tan delta were more pronounced at higher concentrations of the block copolymers on the surface. The same trend is discernible in the flexural data, although it is not as pronounced.

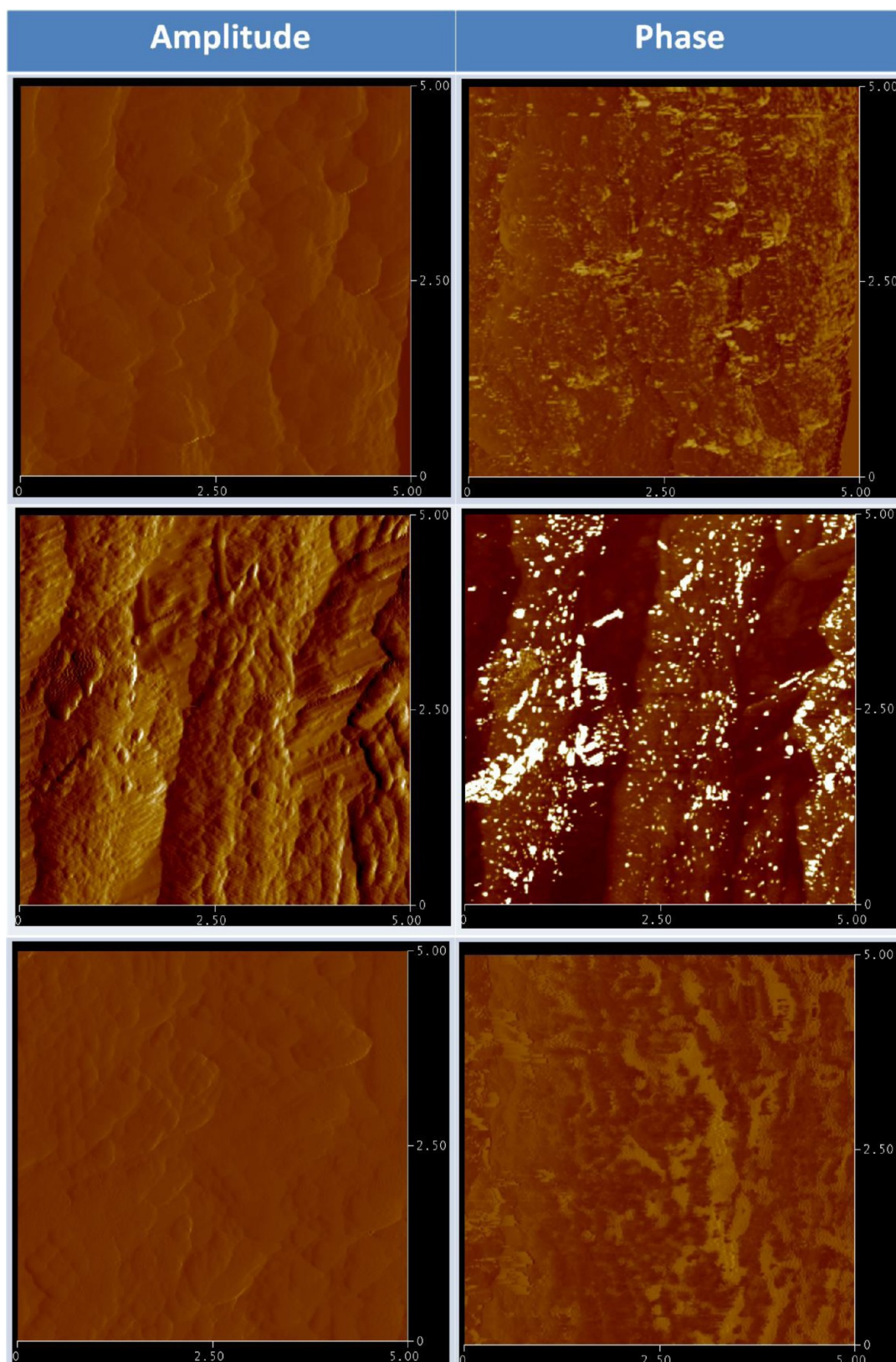


**Figure 4.** AFM amplitude and phase images (tapping mode, 5 micrometers scan areas) for the alkali-treated jute, alkali-treated jute followed by surface adsorption with solution S<sub>1</sub> or solution S<sub>2</sub> (top to bottom, respectively).

The ability of the material to absorb impact is controlled by the toughness of the matrix, the tensile properties of the fibers and the interfacial properties.<sup>7</sup> The impact properties (using the edgewise Charpy test methodology) of the biocomposites

presented in Figure 7 show that the surface treatment of the jute substrate had a noticeable effect.

It has also been shown that the energy absorption of these types of materials can be correlated to the microfibril angle of

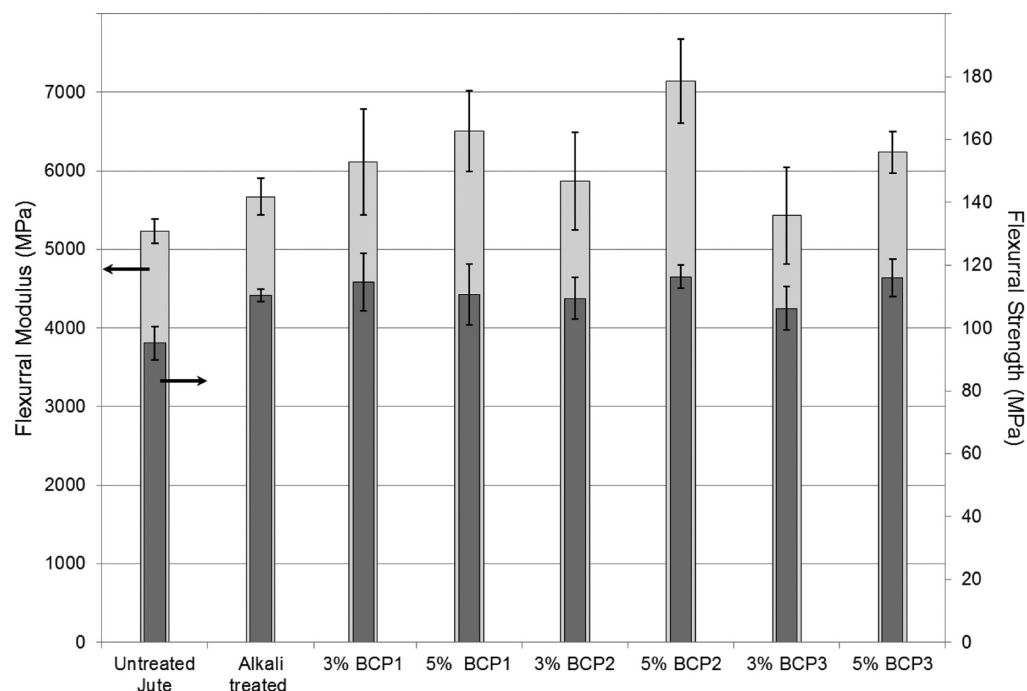


Figure 5. Flexural properties of the poly lactide biocomposites.

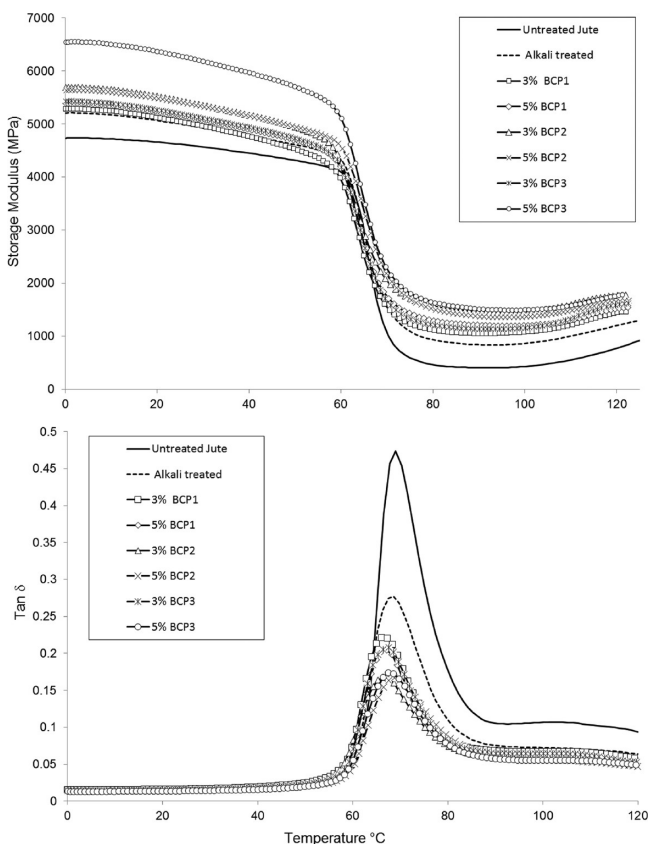


Figure 6. Storage modulus ( $E'$ ) and loss tangent ( $\tan \delta$ ) of the biocomposites reinforced with untreated, alkali-treated, and alkali-treated followed by block copolymer surface adsorption, jute fibrous substrate.

the fibrous component; more specifically any increase in microfibril angle will lead to an increase in elongation at break of the fiber which will consequently have a positive effect on the

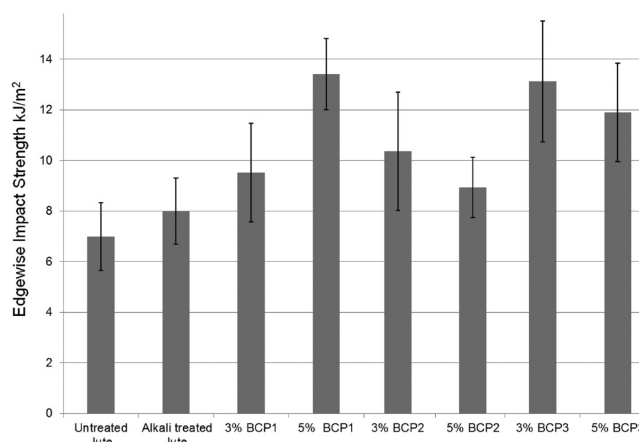
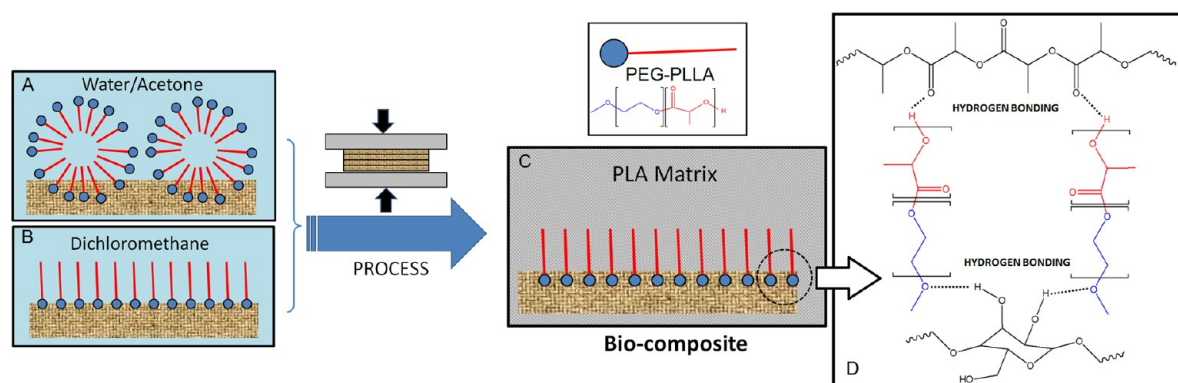


Figure 7. Edgewise Charpy impact strength of the biocomposites.

impact strength.<sup>9,12,34</sup> It has been aforementioned that in this work the elongation at break of the fibers increased after alkali treatment and it has also been demonstrated that interfacial properties of the composites were improved after surface treatment. This suggests that the micromechanisms of failure during impact testing were influenced by both these factors, which positively contributed to the increase in energy absorption through effective resistance to crack propagation. SEM images (see the Supporting Information, S14) of the fractured surfaces after impact testing also suggested improved poor fiber–matrix adhesion.

**Intercorrelation between Interface and Properties.** Up to this point, we have demonstrated that surface adsorption of amphiphilic PEG-PLAA copolymers of various hydrophobic/hydrophilic ratios is very effective in improving the physical performance of jute/PLA biocomposite. Here we attempt to provide a deep understanding and interpretation of the nature of the interactions at the fiber–matrix interface, which is



**Figure 8.** Idealized molecular organization of the block copolymers at the cellulosic interface after surface adsorption in (A) water/acetone and (B) dichloromethane. (C) During processing, molecular re-organization of the amphiphilic block copolymers upon changes in surface hydrophilicity is proposed. (D) The hydrogen bonding interactions at the solid–solid interface are described on the right hand side.

paramount to fully understand the mechanism responsible for the changes in properties.

First, the results indicated that surface adsorption of the BCP2 from dichloromethane induced the deposition of PEG-PLLA monolayer on the surface of the fibers. After removal of the solvent, the block copolymer BCP2 was most likely organized onto the surface possibly in an upright position fashion where in this configuration, the PEG blocks interact with the hydrophilic substrate (Figure 8B). In this particular configuration, the PLLA hydrophobic tails are free and are in a favorable arrangement to interact with the diffusing polylactide matrix molecules during the fabrication process.

Conversely, surface adsorption of the BCP1 and BCP3 block from water/acetone mixtures was shown to induce the deposition of spherical micelles with an inner PLLA core (Figure 8A). In this particular configuration, the PEG molecules are exposed, rendering the surface more hydrophilic. Keeping in mind that the surrounding polylactide matrix is hydrophobic, it is important to stress that this particular arrangement does not seem to be favorable in compatibilizing the interface. Nonetheless, the experimental results indicated differently, showing a clear enhancement in performance and interfacial properties even after deposition of BCP1 and BCP3. The changes in the environment surrounding the block copolymers during processing are believed to be responsible for the trends. The block copolymers are, during processing at 175°C, in their amorphous state (as they are well above their melting temperature) and the nature of the self-assembly is most likely lost. Nonetheless, as the PLA molecules (of the matrix) diffused through the interface, the environment surrounding the block copolymers changed to become hydrophobic. During the early stage of the processing when no pressure was applied and when molecular diffusion in the melt was not restricted, it is proposed that molecular reorganization presumably into a monolayer configuration occurred, favoring the interactions with both the hydrophilic fibers and hydrophobic polylactide matrix (Figure 8C). It is not the first time molecular reorganization upon changes in surface hydrophilicity has been reported. It has been described elsewhere in the particular case of a cross-linked hyperbranched fluoropolymer and linear PEG amphiphilic network.<sup>27,35</sup> It is suggested that the enhancement in properties displayed by the bio-composites are most likely derived from strong interactions such as intra and inter-molecular hydrogen bonds formed across the fiber-matrix interface (Figure 8D). It is, however,

important to point out that we are purely stipulating a hypothesis to understand the mechanism responsible for the changes in properties; some work is currently under way to confirm this theory.

## CONCLUSIONS

This work brought some insight into the successful interfacial property enhancement in a jute and polylactide bio-composite by surface compatibilization with an amphiphilic and biodegradable poly (ethylene glycol)-*b*-poly(L-lactide) (PEG-PLLA) block copolymer. The deposition from solution and surface adsorption onto the cellulosic substrate of PEG-PLLA copolymers having various hydrophobic/hydrophilic ratios leads to a notable improvement in the flexural, thermomechanical, and impact performance of the corresponding biocomposite materials with a polylactide matrix. The findings of the study also showed that the surface concentration of the block copolymers had an overpowering effect over the hydrophobic/hydrophilic ratio. A theoretical arrangement mechanism of the block copolymers onto the jute substrate during deposition (at the liquid–liquid interface) and after fabrication of the bio-composites using a compression molding process (at the solid–solid interface) has been proposed. The improvements in performance have been attributed to the hydrogen bonding interactions at the interface between the jute fibers and the poly (ethylene glycol) block. Although the results reported here are confined to one type of ligno-cellulosic fiber (i.e. jute), this concept is unique as it shows that, by tuning the amphiphilicity and the type of building blocks, it is possible to control the surface properties of natural fibers by self-assembly and disassembly of the amphiphiles for functional biomaterials. We are currently investigating other types of copolymers and their effects on the interfacial and physical properties of natural fiber reinforced biopolymer composites. At the very least, the method presented here offers a potentially cleaner alternative to other chemical methods presented in the literature, preserving the biodegradable nature of the fibers.

## ASSOCIATED CONTENT

### Supporting Information

<sup>1</sup>H NMR data used to estimate the molecular weight of the synthesized copolymers is available in the supporting information (SI1). The gas phase chromatography data in supporting information (SI2) shows that the polylactide matrix did not undergo hydrolysis during the processing conditions

described in the experimental section. SEM surface characterization the jute fibers and fractured samples after impact testing are available in the supporting information (SI3 and SI4). This material is available free of charge via the Internet at <http://pubs.acs.org>

## AUTHOR INFORMATION

### Corresponding Author

\*E-mail: [kmagn@deakin.edu.au](mailto:kmagn@deakin.edu.au).

### Notes

The authors declare no competing financial interest.

## ACKNOWLEDGMENTS

The authors thank Alfred Deakin Prof. Xungai Wang at Deakin University for financial support of this research project. The authors gratefully acknowledge the helpful assistance of Mr. Shuhua Peng for the GPC measurement.

## REFERENCES

- (1) O'Donnell, A.; Dweib, M. A.; Wool, R. P. *Compos. Sci. Technol.* **2004**, *64*, 1135–1145.
- (2) Suddell, B. C.; Evans, W. J. Natural Fiber Composites in Automotive Applications. In *Natural Fibers, Biopolymers, and Biocomposites*; Mohanty, A. K., Manjusri, M., Lawrence, T. D., Eds.; CRC Press: Boca Raton, FL, 2005; p 16.
- (3) Krawczak, P. Bioplastics and Vegetal Fibre Reinforced Bioplastics in Automotive Applications. In *Handbook of Bioplastics and Biocomposites Engineering Applications*; Pilla, S., Ed.; Wiley: New York, 2011; p 397.
- (4) Oksman, K.; Skrifvars, M.; Selin, J. F. *Compos. Sci. Technol.* **2003**, *63*, 1317–1324.
- (5) Joseph, K.; Varghese, S.; Kalaprasad, G.; Sabu, T.; Prasannakumari, L.; Koshy, P.; Pavithran, C. *Eur. Polym. J.* **1996**, *32*, 1243–1250.
- (6) Satyanarayana, K. G.; Arizaga, G. G. C.; Wypych, F. *Prog. Polym. Sci.* **2009**, *34*, 982–1021.
- (7) Bledzki, A. K.; Gassan, J. *Prog. Polym. Sci.* **1999**, *24*, 221–274.
- (8) Kafi, A. A.; Magniez, K.; Fox, B. L. *Compos. Sci. Technol.* **2011**, *71*, 1692–1698.
- (9) Graupner, N. *J. Mater. Sci.* **2008**, *43*, 5222–5229.
- (10) Graupner, N. *J. Compos. Mater.* **2009**, *43*, 689–702.
- (11) Graupner, N.; Herrmann, A. S.; Müssig, J. *Compos., Part A* **2009**, *40*, 810–821.
- (12) Graupner, N.; Müssig, J. *J. Biobased Mater. Bioenergy* **2009**, *3*, 249–261.
- (13) Plackett, D.; Løgstrup, A. T.; Batsberg, P. W.; Nielsen, L. *Compos. Sci. Technol.* **2003**, *63*, 1287–1296.
- (14) Huda, M. S.; Drzal, L. T.; Mohanty, A. K.; Misra, M. *Compos. Sci. Technol.* **2008**, *68*, 424–432.
- (15) Hu, R.; Lim, J. K. *J. Compos. Mater.* **2007**, *41*, 1655–1669.
- (16) Hu, R. H.; Sun, M. Y.; Lim, J. K. *Appl. Mater. Res.* **2010**, *31*, 3167–3173.
- (17) John, M. J.; Bellmann, C.; Anandjiwala, R. D. *Carbohydr. Polym.* **2010**, *82*, 549–554.
- (18) Liang, S.; Wu, J.; Tian, H.; Zhang, L.; Xu, J. *ChemSusChem* **2008**, *1*, 558–563.
- (19) Huson, M.; Evans, D.; Church, J.; Hutchinson, S.; Maxwell, J.; Corino, J. *Struct. Biol.* **2008**, *163*, 127–136.
- (20) Sarkar, P. B.; Mazumdar, A. K.; Pal, K. B. *J. Text. Inst., Trans.* **1948**, *39*, 44–58.
- (21) Mwaikambo, L. Y.; Ansell, M. P. *J. Appl. Polym. Sci.* **2002**, *84*, 2222–2234.
- (22) Gassan, J.; Bledzki, A. K. *J. Appl. Polym. Sci.* **1999**, *71*, 623–629.
- (23) Ray, D.; Sarkar, B. K. *J. Appl. Polym. Sci.* **2001**, *80*, 1013–1020.
- (24) Mukherjee, A.; Ganguly, P. K.; Sur, D. *J. Text. Inst.* **1993**, *84*, 348–353.
- (25) Dai, Z.; Piao, L.; Zhang, X.; Deng, M.; Chen, X.; Jing, X. *Colloid Polym. Sci.* **2004**, *282*, 343.
- (26) Yamamoto, Y.; Yasugi, K.; Harada, A.; Nagasaki, Y.; Kataoka, K. *J. Controlled Release* **2002**, *82*, 359–371.
- (27) Ruan, G.; Feng, S.-S. *Biomaterials* **2003**, *24*, 5037–5044.
- (28) Grant, C. D.; DeRitter, M. R.; Steege, K. E.; Fadeeva, T. A.; Castner, E. W. *Langmuir* **2005**, *21*, 1745–1752.
- (29) Ahmad, S. H.; Rased, R.; Bonnia, N. N.; Zainol, I.; Mamun, A. A.; Bledzki, A. K.; Beg, M. D. H. *J. Compos. Mater.* **2011**, *45*, 203–217.
- (30) Yan, L.; Yiu-Wing, M.; Lin, Y. *Compos. Interfaces* **2005**, *12*, 141–163.
- (31) Rozman, H. D.; Saad, M. J.; Ishak, M. Z. A. *Polym. Test.* **2003**, *22*, 335–341.
- (32) Rong, M. Z.; Zhang, M. Q.; Liu, Y.; Yang, G. C.; Zeng, H. M. *Compos. Sci. Technol.* **2001**, *61*, 1437–1447.
- (33) Aziz, S. H.; Ansell, M. P. *Compos. Sci. Technol.* **2004**, *64*, 1219–1230.
- (34) Miecz, K. P.; Reussmann, T.; Hauspurg, C. *Materialwiss. Werkstofftech.* **2000**, *31*, 169–174.
- (35) Gudipati, C. S.; Greenlief, C. F.; Johnson, J. A.; Prayongpan, P.; Wooley, K. L. *J. Polym. Sci., Part A: Polym. Chem.* **2004**, *42*, 6193–6208.